Motional Stark effect on bound-free spectra

Thomas A. Gomez
Department of Astrophysical and Planetary Sciences, University of Colorado Boulder, Boulder, Colorado 80305, USA;
National Solar Observatory, University of Colorado Boulder, Boulder, Colorado 80303, USA;
and Department of Astronomy, University of Texas at Austin, Austin, Texas 78712, USA

Mark C. Zammit and Christopher J. Fontes
Los Alamos National Laboratory, Los Alamos, New Mexico 87545, USA

Igor Bray
Department of Physics and Astronomy, Curtin University, Perth, Western Australia 6845, Australia

Jackson White
Department of Astronomy, University of Texas at Austin, Austin, Texas 78712, USA
and Computational Physics Division, Los Alamos National Laboratory, Los Alamos, New Mexico 87545, USA

(Received 14 June 2024; accepted 19 August 2024; published 10 September 2024)

The motion of atoms through a magnetic field (due to a change in reference frame) will result in an additional electric field felt by the electrons in that atom. The motional Stark effect is a well-established effect that has been approximately included in calculations of spectra of magnetized plasmas, usually through diagonalizing the Hamiltonian. The motional Stark effect for continuum states is poorly defined due to an overlap integral that results in a Dirac delta function. This paper presents a workaround by evaluating the motional Stark effect in the Green's function within the scattering formalism. We report on some results pertaining to bound-free spectra for white dwarf and neutron star magnetic field strengths. In most cases, resonances in the continuum are shifted and broadened. This behavior has the effect of raising the Rosseland mean opacity in white dwarfs and neutron star atmospheres.

DOI: 10.1103/PhysRevA.110.032808

I. INTRODUCTION

In a large magnetic field, it is well established [1] that the internal electronic states are linked with the motion of the atom through space. This connection manifests as a motional Stark effect term in the Hamiltonian of the atom

$$H_{\mathrm{MSE}} = \vec{v}_{\mathrm{atom}} \cdot (\vec{B} \times \vec{r}), \tag{1}$$

where $\vec{v}_{\mathrm{atom}}$ is the velocity of the atom and $\vec{r}$ is the dipole moment of the electrons inside the atom. The motional Stark effect can be derived from a simple transformation of a static (i.e., laboratory) reference frame to the moving atomic reference frame. It can also be rigorously derived from separating the multiparticle Hamiltonian into its center of mass and relative coordinates [2], as is commonly done in atomic problems [3].

It is not possible to fully separate the center of mass and relative coordinates; often a pseudoseparation is used and then the atomic structure is corrected using perturbation theory [4–6]. These corrections shift the energies of the levels, which leads to a broadening of spectral lines in the atmospheres of stars with high magnetic fields [5,7,8].

There are some complications regarding the motional Stark effect. One such example is interference with particle collisions [9]. More important is that an extension from discrete to continuum states does not exist; this issue is the focus of this paper. The application of calculating continuum states with the motional Stark effect is relevant for calculations of bound-free opacity, as well as in collision problems [10,11].

The complication with continuum states lies with the boundary condition of continuum states as well as the form of Eq. (1). Continuum states are notoriously complicated due to their wave functions normalizing to a delta function. The evaluation of matrix elements of Eq. (1) for a continuum function results a delta function. One way around this complication is to volume normalize the wave function [12], but this option is not satisfactory due to the modification of the normalization properties of continuum wave functions.

The bound-free continuum contribution provides an important opacity source when calculating the spectra of magnetized plasmas. It is essential, especially for diagnostic purposes and for calculating atmospheric structure, to accurately calculate the bound-free opacity. There is no simple analytic prescription to calculate the bound-free opacity in a high magnetic field, only numerical techniques can be used. Further, the continuum is filled with resonances [13] and the free states are quantized into Landau levels.

It is well known that broader spectral lines lead to an increase of the Rosseland mean opacity, an important quantity for radiation transport. Since the motional Stark effect is known to broaden and shift spectral lines, its inclusion in opacity calculations can result in changes to average opacities.

In this paper, we explore the impact that the motional Stark effect has on continuum functions. The rest of the paper is organized as follows. Section II reviews atomic wave functions in the presence of a large magnetic field. Section III further details the problems associated with trying to calculate the motional Stark effect for continuum problems. We resolve this problem in Sec. IV by using a Green's function to tackle continuum problems. We present results in Sec. V, showing how the motional Stark effect can impact bound-free spectra. We discuss important aspects about opacity in Sec. VI, focusing on both Rosseland mean opacities and oscillator strength sum rules. Our conclusions are presented in Sec. VII.

II. CONSTRUCTION OF WAVE FUNCTIONS IN A MAGNETIC FIELD

It is common to use cylindrical coordinates to solve for the motion of an electron in a high magnetic field. In the absence of a nuclear potential

$$H_0 = \frac{1}{2m_e}(\vec{p} - e\vec{A}(r))^2 \tag{2}$$

$$= \frac{1}{2m_e}\left[p^2 - e\vec{p}\cdot\vec{B}\times\vec{r} + \frac{1}{4}(\vec{B}\times\vec{r})^2\right], \tag{3}$$

where the symmetric gauge is assumed, an exact solution can be found. A free electron wave function can be described under these conditions by the quantum numbers $|knm\rangle$, where k is the linear momentum in the z direction (aligned with the magnetic field) and nm are the radial and azimuthal quantum numbers, respectively. The wave function in this case is separable, i.e.,

$$\langle r|kn_\varrho m\rangle = g_k(z)\Phi_{n_\varrho m}(\varrho, \varphi), \tag{4}$$

with energies

$$E_{kn_\varrho m} = \frac{1}{2}k^2 + \frac{|e|\beta}{2}(2n_\varrho + |m| + m + 1) \tag{5}$$

in atomic units. In the previous expression, β is the magnitude of the magnetic field in atomic units, i.e., $\beta = B/B_0$ where $B_0 = 2.35 \times 10^5$ T. The part of the wave function in the z direction, denoted here by $g_k(z)$, is often referred to as the longitudinal wave function. The wave functions $\Phi_{n_\varrho,m}(\varrho, \varphi)$ are what is known as Landau wave functions [1,2,10,14], and they describe the behavior of the electron perpendicular to the magnetic field.

The nm basis is particularly advantageous for Coulomb problems. Another basis set that can be used takes advantage of the (infinite) degeneracy of the energy eigenvalues with respect to the m quantum number. In this case, the new quantum numbers are n and s, where [15]

$$n = n_\varrho + \frac{1}{2}(|m| + m), \tag{6}$$

$$s = n_\varrho + \frac{1}{2}(|m| - m), \tag{7}$$

$$E_{kns} = \frac{1}{2}k^2 + \frac{|e|\beta}{2}(2n + 1), \tag{8}$$

In the presence of a nuclear potential, a solution of the form displayed in Eq. (11) below is not possible since the spherically symmetric nuclear potential breaks the cylindrical symmetry. There are multiple ways of calculating atomic wave functions in high magnetic fields. One of the most common methods is to build wave functions as a linear combination of cylindrical wave functions [16], i.e.,

$$\left[\frac{1}{2}\frac{d^2}{dz^2} - V^{\text{eff}}_{n_\varrho m, n_\varrho m}(z) + E - E_{n_\varrho m}\right]g_{\nu n_\varrho m}(z) = \sum_{n'_\varrho m'} V^{\text{eff}}_{n_\varrho m, n'_\varrho m'}(z)\, g_{\nu n'_\varrho m'}(z), \tag{9}$$

where the effective nuclear potentials are given by

$$V^{\text{eff}}_{n_\varrho m, n'_\varrho m'} = -\iint d\varrho\, d\varphi\, \varrho\, \Phi_{n_\varrho m}(\varrho, \varphi)\frac{Z}{\sqrt{\varrho^2 + z^2}}\Phi_{n'_\varrho m'}(\varrho, \varphi). \tag{10}$$

Here, we use the quantum number ν to denote a bound state and k continues to designate continuum states. The construction of Eq. (10) is based on the assumption that the magnetic field dominates, creating the $E_{n_\varrho m}$ term, which is the second term of Eq. (5). For continuum states, the most basic solution is what is known as the "adiabatic" solution, where a continuum wave function is represented by

$$|f\rangle = |kn_\varrho m\rangle. \tag{11}$$

The nonadiabatic solution

$$|f\rangle = \sum_n c_n |kn_\varrho m\rangle \tag{12}$$

is a linear combination of states that can be built up from a reactance matrix [17]. These reactant matrices (and later S matrices) are used to calculate autoionizing resonances in the continuum [18]. The total continuum wave function is expressed explicitly as [19–21]

$$|f\rangle = |kn_\varrho m\rangle + \sum\!\!\!\!\!\!\int_{k'n'_\varrho m'} |k'n'_\varrho m'\rangle\langle k'n'_\varrho m'|\mathcal{G}T(E_{kn_\varrho m})|kn_\varrho m\rangle; \tag{13}$$

the Appendix provides a brief overview of the scattering problem and an explanation of the symbols $\mathcal{G}T(E_{kn_\varrho m})$ that appear in the above equation.

An example of using Eq. (11) versus Eq. (13) for bound-free oscillator strengths is demonstrated in Fig. 1. Oscillator strengths for bound-free or free-free transitions are often denoted in differential form, such as

$$\frac{df}{dE} \quad \text{or} \quad \frac{df}{d\omega}, \tag{14}$$

with the first denoting the ejected electron energy and the second the photon energy. There are other normalizing conventions, such as using the momentum of the ejected particle. However, since our concern here is with the spectrum, using Eq. (14) is the most convenient form to present the results. The second solves Eq. (9) exactly using scattering methods, while the first neglects the right-hand side of Eq. (9). This example is for H I at $B = 400$ MG, a magnetic field that was observed in white dwarf atmospheres. Using the single-state approximation, the wave functions exhibit an expected featureless continuum with distinct thresholds for the different Landau levels. The exact solution reveals the presence of resonances, which now dominate the continuum spectrum. The calculations for Fig. 1 were obtained by truncating the number

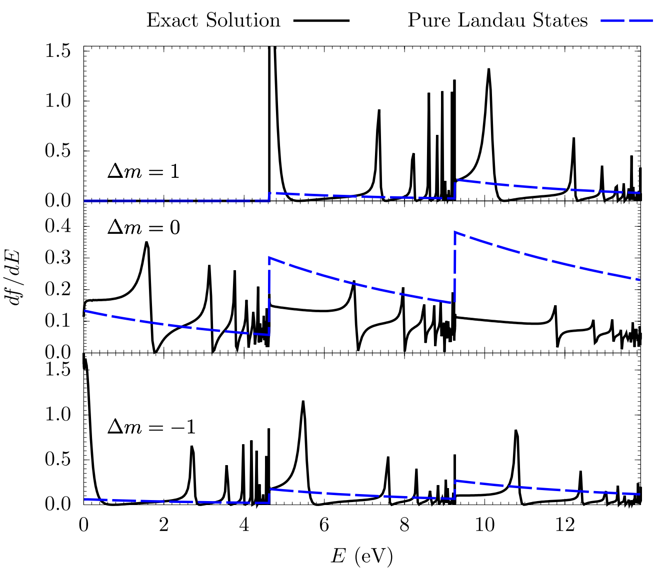

FIG. 1. Comparison of the bound-free oscillator strengths (df/dE) obtained with different treatments of the continuum as a function of the ejected electron energy. Dashed blue lines use Eq. (11) and solid black lines are calculated using the exact solution constructed from Eq. (13). Calculations performed for H I in a $B = 400$ MG ($\beta = 0.17$) field. The exact solution results in the continuum spectrum being dominated by resonances.

of quantum states, including only up to $n_\varrho = 3$. These features are expected, as was found previously in Zhao *et al.* [13].

III. CONTINUUM WAVE FUNCTIONS WITH A MOVING ATOM

The equations in Sec. II centered around the assumption that the central nucleus of the atom is infinitely massive, i.e., it is static. There are a number of consequences of not having an infinitely massive nucleus. For example, there is a shifting of atomic energies that depends on the finite mass of the atom [22] even without the atomic motion. The energy-level structure becomes even more complicated with atomic motion.

When the atom is moving, additional terms appear in the Hamiltonian due to the motional Stark effect. For the case of an H-like atom we have [2]

$$H_{\mathrm{MSE}} = -\frac{1}{M}\frac{1 + Zm_e/m_N}{1 + m_e/m_N}\Pi_s \cdot (\beta \times r), \tag{15}$$

where

$$\Pi_s = \nabla_R - \frac{Z-1}{2}\beta \times R, \tag{16}$$

m_e, m_N, and M are the electron, nuclear, and total masses, Z is the charge of the nucleus, and R is the position operator of the center-of-mass coordinate. The matrix elements for the motional Stark effect [Eq. (15)] involve a cross product of the position operator with the magnetic field, the resulting vector operator (which is dotted in with the velocity vector) is nonzero only perpendicular to the magnetic field. Therefore, the only position operator matrix elements that need to be evaluated are perpendicular to the magnetic field. The evaluation of these matrix elements involves an overlap integral in the z direction. For bound states, this becomes

$$\langle \nu n_\varrho m|r_\perp|\nu' n'_\varrho m'\rangle = \langle n_\varrho m|r_\perp|n'_\varrho m'\rangle\langle \nu|\nu'\rangle, \tag{17}$$

and presents no numerical issues because the longitudinal wave functions decay to zero as $|z| \to \infty$. Bezchastnov and Pavlov [6] calculated the ion cyclotron transitions of the He^+ ion with full consideration of the motional Stark effect connecting the center-of-mass motion with the electronic motion. However, for continuum problems, continuum wave functions oscillate at large z, and the overlap integral $\langle k|k'\rangle$ becomes a delta function. In this case the wave functions are usually normalized according to

$$\langle kn_\varrho m|k' n'_\varrho m'\rangle = \delta_{mm'}\delta_{n_\varrho n'_\varrho}\delta(k-k')e^{i\sigma}. \tag{18}$$

This result is obtained by recognizing that at large $|z|$, the longitudinal part of the wave function of a continuum state is defined by the term

$$\frac{1}{\sqrt{2\pi}}e^{\pm ikz + i\sigma_{n_\varrho m}}, \tag{19}$$

where $\sigma_{n_\varrho m}$ is a phase shift due to traveling through a potential, which in this case is a nuclear potential, and

$$\sigma = \sigma_{n_\varrho m} - \sigma_{n'_\varrho m'}, \tag{20}$$

is the total phase shift, analogous to the Coulomb phase shift, and is factored out when evaluating Eq. (18). It is convenient to use the symmetric and antisymmetric basis, which allows for purely real arithmetic. The resulting overlaps are

$$\langle k_+|k'_+\rangle = \delta(k-k')\cos(\sigma)\,;\ \langle k_-|k'_-\rangle = \delta(k-k')\cos(\sigma), \tag{21}$$

where the $+$ and $-$ subscripts indicate the use of symmetric and antisymmetric wave functions, respectively.

One way to get around the difficulty of evaluating the overlaps in Eq. (21) is to use a different center for the atomic problem, using a shifted center of symmetry [7,23]. In the first, the motional Stark term disappears, but then one is left to calculate interaction potentials in a displaced basis set, where m is no longer a good quantum number, presenting a different set of problems, and having to explicitly solve for the proton wave function relative to the guiding center.

In Potekhin [12], the continuum wave functions were forced to be normalized to unity inside some length in the z direction, L_z. Making this choice produces the normalization condition

$$\iint d\varrho d\varphi \int_{-L_z/2}^{L_z/2} dz|\psi_{kn_\varrho m}(z,\varrho,\varphi)|^2 = 1. \tag{22}$$

This expression is mathematically convenient to evaluate, but is inconvenient due to the resulting wave functions no longer being normalized as a true continuum function, though the authors of Ref. [12] claimed that in the limit that $L_z \to \infty$, it does approach the correct limit. Rather than taking the limit, a more fundamental approach is desirable, and would aid in its inclusion in collision and line-broadening problems [10,11].

IV. USING GREEN'S FUNCTIONS FOR THE MOTIONAL STARK EFFECT IN CONTINUUM PROBLEMS

The primary challenge with continuum problems is that the overlap integral in Eq. (17) as written results in a delta function when it is applied to continuum states. We consider several ways to get around the issue of the delta function, including changing the order of solutions and looking for an alternate form of the matrix element. The successful method that we will present here is to use the Green's function within the scattering formalism.

A. Green's function including motional Stark

The technique that we propose here involves the use of Green's functions within the scattering formalism [19,20]; Appendix gives a brief overview of scattering, including how to address systems with two potentials.

Due to the delta function in the matrix elements of V_{MSE} (see the discussion in the previous section), it makes sense to couple the resulting delta functions with the other operator that contains a delta function, i.e., the Green's function. We define a Green's function that includes the motional Stark operator V_{MSE},

$$\mathcal{G} = \frac{1}{E - H_0 - H_{\mathrm{MSE}}} \tag{23}$$

$$= \frac{1}{1 - (E - H_0)^{-1} H_{\mathrm{MSE}}} \frac{1}{E - H_0}, \tag{24}$$

where H_0 is the Hamiltonian without the motional Stark term. This expression can be rearranged to write the total Green's function as an integral equation

$$\mathcal{G} = \mathcal{G}_0 + \mathcal{G}_0 H_{\mathrm{MSE}} \mathcal{G}, \tag{25}$$

where $\mathcal{G}_0 = (E - H_0)^{-1}$ and has analytic properties in the $|kn_\varrho m\rangle$ basis. The complete Green's function can be solved using the close-coupling equations as defined in Ref. [24], i.e.,

$$[1 - \mathcal{G}_0 H_{\mathrm{MSE}}]\mathcal{G} = \mathcal{G}_0, \tag{26}$$

where, in matrix element form,

$$\sum_{n'm'} \int dk' \delta(k - k')[\delta_{nn'}\delta_{mm'} - \mathcal{G}_{0,knm}\langle nm|H_{\mathrm{MSE}}|n'm'\rangle] \times \langle k'n'm'|\mathcal{G}|knm\rangle = \mathcal{G}_{0,knm}, \tag{27}$$

where the phase shift in Eq. (18) is implied and we use a more compact notation for the Green's function due to the fact that it is diagonal in our chosen basis. Here, the delta function is factored out and is now part of the integral. The integral is now readily performed

$$\sum_{n'm'} [\delta_{nn'}\delta_{mm'} - \mathcal{G}_{0,knm}\langle nm|H_{\mathrm{MSE}}|n'm'\rangle]\langle kn'm'|\mathcal{G}|knm\rangle = \mathcal{G}_{0,knm}. \tag{28}$$

From this result, it is clear that the Green's function is diagonal in the z linear momentum, but not in the radial or azimuthal quantum numbers.

An alternate formulation of the Green's function can fully separate it into a noninteracting part and an interacting part. The interaction term can be put within a T matrix

$$\mathcal{G} = \mathcal{G}_0 + \mathcal{G}' = \mathcal{G}_0 + \mathcal{G}_0 \mathcal{T}_{\mathrm{MSE}}(E)\mathcal{G}_0, \tag{29}$$

where

$$\mathcal{T}_{\mathrm{MSE}}(E) = \frac{1}{1 - H_{\mathrm{MSE}}(E - H_0)^{-1}} H_{\mathrm{MSE}}, \tag{30}$$

which describes only the T matrix resulting from the motional Stark effect. The T matrix can be obtained using the close-coupling technique

$$[1 - H_{\mathrm{MSE}}(E - H_0)^{-1}]\mathcal{T}_{\mathrm{MSE}}(E) = H_{\mathrm{MSE}}, \tag{31}$$

and can be solved using matrix solve routines (i.e., $Ax = b$) as was done in Ref. [24]. The matrix element of this equation will likewise have overlap integrals of the z component

$$\sum_{n'm'} \int dk' \delta(k - k')[\delta_{nn'}\delta_{mm'} - \langle nm|H_{\mathrm{MSE}}|n'm'\rangle \mathcal{G}_{0,k'n'm'}] \times \langle k'n'm'|\mathcal{T}_{\mathrm{MSE}}(E)|k''n''m''\rangle = \langle nm|H_{\mathrm{MSE}}|n''m''\rangle \delta(k - k''). \tag{32}$$

It is already known from Eqs. (28) and (29) that the resulting T matrix has to also be diagonal in the z linear momentum, k. We can then introduce a delta function as part of the definition of the T matrix, and perform the integral over k', to obtain the reduced equation

$$\sum_{n'm'} [\delta_{nn'}\delta_{mm'} - \langle nm|H_{\mathrm{MSE}}|n'm'\rangle \mathcal{G}_{0,k'n'm'}] \times \langle k'n'm'|\mathcal{T}_{\mathrm{MSE}}(E)|k''n''m''\rangle \delta(k - k'') = \langle nm|H_{\mathrm{MSE}}|n''m''\rangle \delta(k - k''). \tag{33}$$

This equation can be solved by simply ignoring the delta functions, as long as they are included when solving for the final quantities of interest. This approach poses no problems because Green's functions are evaluated within an integral.

B. Modification of the scattering *T* matrix for collision problems

This new form of the Green's function can now be included in the collision T matrix that is used to describe electron-atom scattering. This T matrix is distinct from $\mathcal{T}_{\mathrm{MSE}}(E)$ because it now includes Coulomb interactions between particles, in this case, the Coulomb interaction between the free electron and the nucleus. The scattering T matrix is defined as

$$T(E) = V + V\mathcal{G}T(E), \tag{34}$$

where V is the off-diagonal nuclear potential, specifically defined to be the right-hand side of Eq. (9), and $\mathcal{G}$ contains the MSE interaction. Since the Green's function is separable into the nonmotional Stark part and motional Stark part [Eq. (28)], we can derive

$$T(E) = V + V(\mathcal{G}_0 + \mathcal{G}')T(E) \tag{35}$$

$$= t(E) + t(E)\mathcal{G}'T(E), \tag{36}$$

where $t(E)$ is the scattering T matrix in the absence of the motional Stark effect

$$t(E) = V + V\mathcal{G}_0 t(E). \tag{37}$$

Finally, we obtain

$$T(E) = \frac{1}{1 - t(E)\mathcal{G}'} t(E), \tag{38}$$

or in a form that isolates the motional Stark contribution

$$T(E) = t(E) + t(E)\mathcal{G}' \frac{1}{1 - t(E)\mathcal{G}'} t(E). \tag{39}$$

For the results presented here, Eq. (34) will be used, though the other forms may prove useful in other contexts.

V. RESULTS

Here we highlight several results to demonstrate the motional Stark effect. The focus here is on the Landau resonances spectrum and bound-free differential oscillator strengths of atomic hydrogen for conditions that are found in astrophysical objects, namely, white dwarfs and neutron stars. The selected cases demonstrate both moderate and strong field effects. Since most cases that we explore here are in thermal plasmas in astrophysical objects, we compare the effect of the motional Stark effect contained within a thermal average.

These conditions cover a range of relative importance between the nuclear interaction and the magnetic field. When $\beta \ll 1$, the nuclear interaction dominates, but, when $\beta \gg 1$, the magnetic field dominates and the electrons are in the Landau regime. The case of $\beta \sim 1$ is an interesting regime where the two interactions are comparable. For the results discussed here, our focus is limited to neutral hydrogen, though the formalism presented above can be easily extended to ionic spectra.

There are a few broad results that apply in all of the cases that we explore here. First, the inclusion of the $\cos(\sigma)$ factor in the evaluation of the matrix element in Eq. (18) does not have significant bearing on the results. To that extent, it appears as if the dominant changes to the spectrum occur in the resonances caused by the highly excited bound states of the atom. This behavior is born out specifically in the neutron star cases where the continuum was largely unaltered by the motional Stark effect. The only part of the spectrum that was modified was in the narrow region of the spectra below the Landau threshold.

Further, the transitions characterized by the $\Delta m = 1$ (i.e., clockwise polarization) selection rule are less affected by the motional Stark effect than the degenerate states. The reason why the clockwise polarization is less susceptible to change from atomic motion is due to the selection rules and energy differences between levels. Analytic expressions for the dipole moment are [1]

$$\langle n+1 m+1 | r_{-1} | nm \rangle = -\sqrt{n+1}/\sqrt{2\beta}, \tag{40}$$

$$\langle nm+1 | r_{-1} | nm \rangle = -\sqrt{n-m}/\sqrt{2\beta}, \tag{41}$$

$$\langle n-1 m-1 | r_{+1} | nm \rangle = -\sqrt{n+1}/\sqrt{2\beta}, \tag{42}$$

$$\langle nm-1 | r_{+1} | nm \rangle = -\sqrt{n-m+1}/\sqrt{2\beta}, \tag{43}$$

where all arguments in the square root need to be zero or greater. This later criterion limits the number of dipole channels that are available to positive m states. For example, the allowed motional Stark channels from $m = 1$ to $m = 0$ will involve states from transitions with either $|\Delta n| = 1$ or more highly excited states with $n > 1$. Therefore, for $m = 1$, the high-energy spectra will be more affected by the motional Stark effect, but low-energy states will be marginally affected, unless the velocities of the atoms are quite high.

The motional Stark effect moves some of the resonances above their respective thresholds. When neglecting the motional Stark effect, there are many resonances just below each Landau threshold. In an electric field, it is well documented [3,25] that some states will lower their energies, and others will have their energies raised and become resonances on the bound-free continuum. It is, therefore, no surprise that the same behavior is reproduced here with the motional Stark effect.

Lastly, for practical application to laboratory and astrophysical objects, the spectra must also be convolved with a thermal Doppler profile. The thermal Doppler broadening will further wash out the details of the resonances. However, in the white dwarf case, the width from thermal Doppler broadening is smaller than the widths of the resonances explored here, so that broadening can be neglected. In the neutron star case, the Doppler broadening is further minimized due to the limited motion perpendicular to the field. At such high magnetic fields, the nucleus and the electrons start spiraling around each other. This behavior increases the effective mass of the atom, thus preventing the occurrence of high velocities, even in the much hotter neutron star atmosphere.

A. H I in white dwarf magnetic fields ($\beta < 1$)

Magnetic fields between 1–1000 MG ($5 \times 10^{-4} \lesssim \beta \lesssim 0.5$) have been found in magnetized white dwarfs [26]. Most white dwarfs have hydrogen in their atmospheres and a much smaller fraction have helium or other heavier elements. Therefore, the study of the hydrogen bound-free continuum will prove valuable to understanding white dwarf spectra.

Figure 2 examines the motional Stark effect in a $B = 400$ MG field ($\beta = 0.17$). Due to the breakdown of selection rules, Fig. 2 indicates the polarization of light, rather than the Δm value that the transition corresponds to. We show results for two different atomic (pseudo)momenta that are common in a white dwarf atmosphere. For such (comparatively) low fields, we neglect the anisotropic mass correction [22], which, for the ground state of hydrogen, does not affect the true velocity of hydrogen to one part in 10^5.

The motional Stark effect has the greatest impact on the number and position of the resonances. We show a zoom in of the resonances below the $n_\varrho = 2$ threshold in the linearly polarized light to more clearly demonstrate the changes due to the motional Stark effect. When we include the motional Stark effect, we average over a thermal distribution of K: the pseudomomentum of the atom. For each K the resonances are both shifted and broadened. Therefore, the thermal average destroys much of the structure that was previously present. This behavior also occurs for the counterclockwise circularly polarized spectra. The clockwise circularly polarized spectra, however, is not as susceptible to the motional Stark effect as the other polarizations. Here the shifting is not as severe but below the first threshold, new resonances appear.

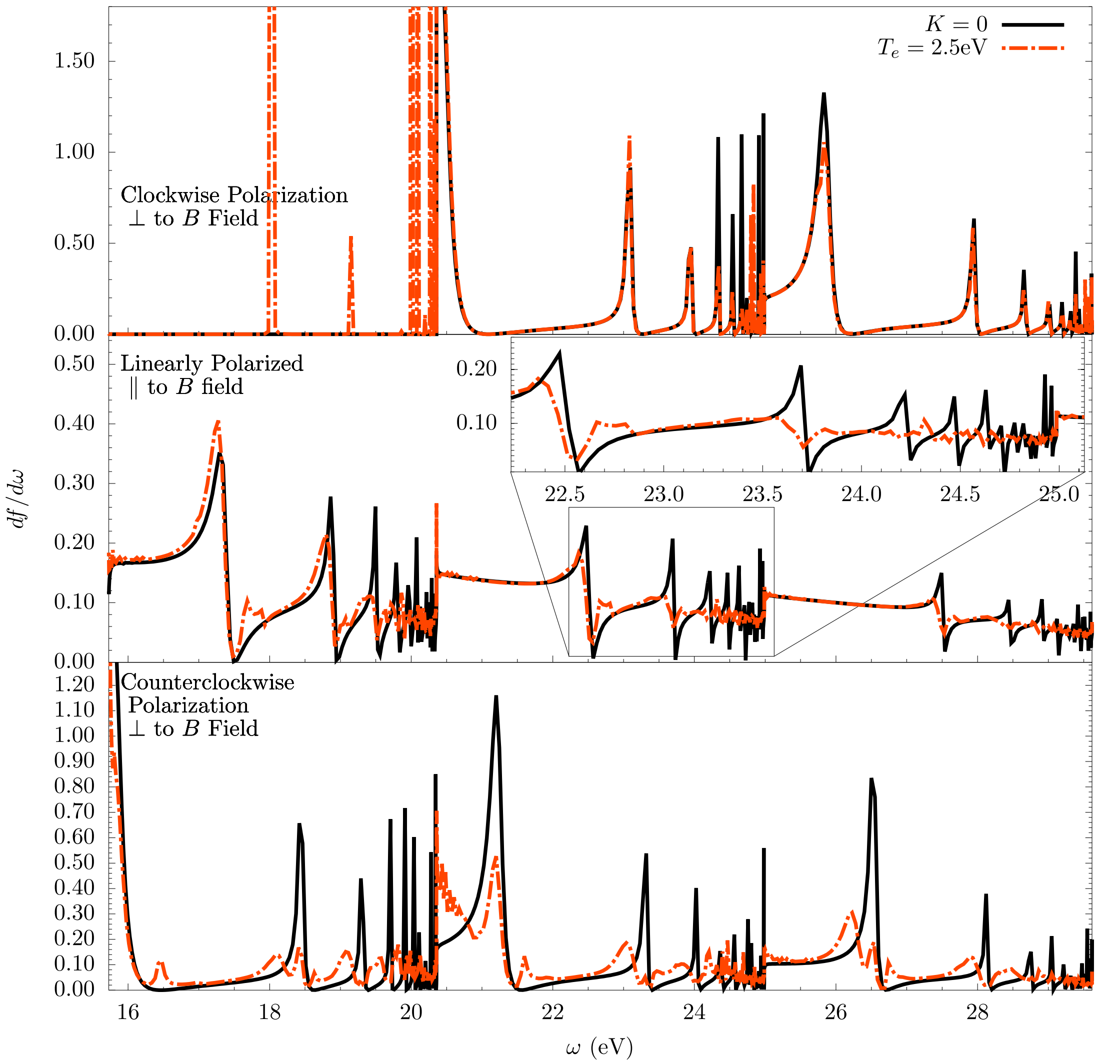

FIG. 2. Examination of the impact of the motional Stark effect on the Lyman spectrum as a function of photon energy with a static hydrogen atom, $K = 0$, and one in a thermal plasma of 2.5-eV temperature with a magnetic field of 400 MG ($\beta = 0.17$). Here, ω is the energy of the photon in eV. The motional Stark effect causes a shifting in the resonances, as well as new resonances to appear. The zoomed-in spectrum demonstrates the shifting and adding of resonances. Additionally, for the clockwise polarization calculation, subthreshold resonances now contribute to the spectrum.

B. H I in neutron star magnetic fields ($\beta > 1$)

For the neutron star case, we explore two magnetic fields, $\beta = 5$ and $\beta = 10^3$. When hydrogen is considered for the latter case, the resulting wave functions are "adiabatic" and are well approximated by Eq. (11). There are some further consequences to the later field that are not considered in the white dwarf case: the finite mass of the proton shifts $m \neq 0$ states by an amount proportional to $-m\beta$. When the magnetic field is large as in the case of neutron star fields, this results in a not-insignificant shift [22]. Therefore, at $\beta = 10^3$, the different m quantum numbers have different energies at which ionization occurs (this is different from ionization energy) in the absence of the motional Stark effect.

This means that the diagonal elements of the T matrix will be extremely small near the $n_\varrho = 0$ threshold since the energies are separated by 10^3 hartrees. The smallness of the T matrix will make it so that the impact of the motional Stark effect cannot be distinguished by the calculation. On one hand, this is a valuable test to verify that the solution does indeed converge and does not diverge like the $r_\perp$ operator does. On the other hand, it makes evaluation of the effect that we are interested in impossible to observe.

We therefore use a modified technique to remedy this situation. The technique requires subtracting a small amount of V^{eff} from the right-hand side of Eq. (9) and including it as part of the T-matrix potential in Eq. (34) so that

$$H_0 = -\frac{1}{2}\frac{d^2}{dz^2} + (1-\alpha)V^{\mathrm{eff}}(z)\delta_{n_\varrho,n'_\varrho}, \tag{44}$$

$$V = -\alpha V^{\mathrm{eff}}(z)\delta_{n_\varrho,n'_\varrho} + V^{\mathrm{eff}}(z)(1-\delta_{n_\varrho,n'_\varrho}), \tag{45}$$

where α is a small number. Using this slightly modified technique, the bound-free spectrum is nearly identical to that

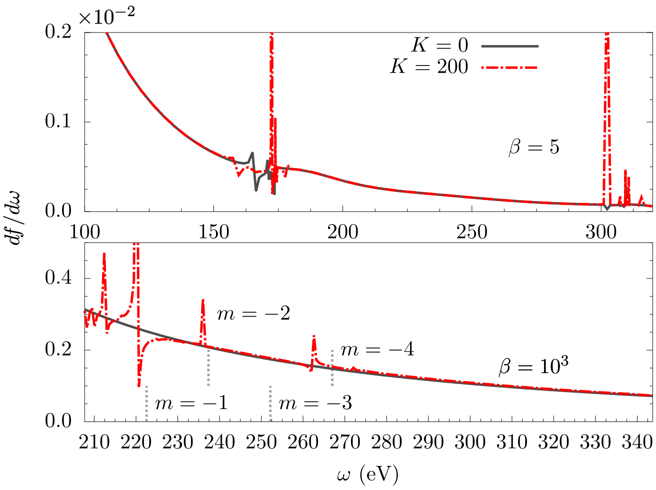

FIG. 3. Linearly polarized photoionization spectrum of H I in $\beta = 5$ (top panel) and $\beta = 10^3$ (bottom panel); photon energy ω is given in eV. Spectra for a static atom are displayed in black and for an atom moving in a hot neutron star atmosphere are displayed in red. Including motional Stark at the high magnetic-field case generates resonances from high energy states of different m, which have now become autoionizing.

for which $\alpha = 0$. As expected, resonances appear when the motional Stark effect is included in the spectrum calculation and these results are independent of the choice of α.

The results here are less interesting than in the white dwarf case because the magnetic field is starting to dominate the electronic behavior. In Fig. 3, we see that, as before, the resonances at $\beta = 5$ are shifted. At $\beta = 10^3$, resonances from the different m thresholds appear and more structure is observed in the bound-free spectrum. Below the next Landau threshold, we see in Fig. 4 that the same qualitative behavior occurs as in the $\beta = 5$ case.

VI. DISCUSSION

Calculations of white dwarf and neutron star spectra depend on getting many of these details correct. Unfortunately, the necessary data (oscillator strengths as a function of photon energy) are not available and approximate solutions [27] are currently the best-available models [28,29]. For magnetic

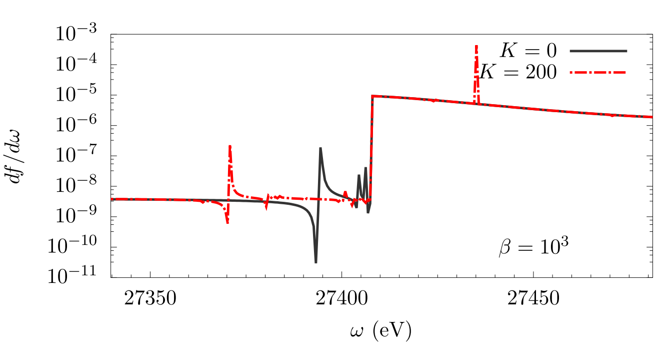

FIG. 4. Same as bottom panel of Fig. 3, but just below the $n_\varrho = 1$ threshold. Extremely high-energy resonances are broadened and reduced. Other resonances have shifted to lower energies.

white dwarfs (for instance), the bound-free opacity is modified in the following way [28]:

$$\kappa_\nu = \frac{\nu}{\nu - \Delta m \nu_L} \kappa_\nu(\nu - \Delta m \nu_L), \tag{46}$$

where ν_L is the shift in the energy levels from the linear Zeeman effect. The resulting opacity will be largely continuous and will not capture any of the resonances presented here. Therefore, the calculations without the motional Stark effect are already much more physical than those already being used by atmosphere models. Nevertheless, as can already be seen by the above results, the motional Stark effect plays an important role in white dwarf atmospheres.

These models may go some way toward resolving a specific problem with magnetic white dwarfs. Schmidt *et al.* [30] and Gänsicke *et al.* [31] reported on white dwarfs with high magnetic fields (∼500 MG) that are quite peculiar, where the visible spectrum is fit with a hotter temperature than the far UV, see Refs. [30,31]. To our knowledge, this problem has yet to be resolved, and cannot be accurately modeled by assuming that the star has a hot spot [31]. Both stars have a sharp change of slope in the UV around 3000 Å, which corresponds to roughly 4.13 eV. This abrupt change roughly corresponds to the Balmer jump in a high magnetic field, similar to the case that we explore above. The UV spectrum measured by Gänsicke *et al.* [31] is relatively featureless, and as we see here, the inclusion of the motional Stark effect on spectrum calculations will aid in smearing out resonances.

It is outside the scope of this particular study to resolve the astrophysical problems presented by Schmidt *et al.* [30] and Gänsicke *et al.* [31]. Such work involves making a grid of these photoionization cross sections. This grid would be quite large, needing to be dependent on not only photon energy, but also magnetic field, photon polarization, and (because the motional Stark effect depends on particle velocities) temperature. Further, white dwarf atmospheres are fairly dense, where plasma perturbations are sure to modify the spectrum even further than what was shown here (all calculations were performed assuming an isolated atomic system), adding yet another dimension to the grid. This hypothetical grid would then need to be incorporated into a stellar atmosphere code, where radiative equilibrium and transport is calculated at a variety of plasma densities and temperatures for a single stellar gravity and effective temperature.

We turn our attention briefly to the evaluation of the mean opacity. A commonly used quantity for evaluating mean opacity is the Rosseland mean [32]

$$\kappa_\nu^{-1} = \frac{\int_0^\infty d\nu \kappa_\nu^{-1} u(\nu, T)}{\int_0^\infty d\nu u(\nu, T)}, \tag{47}$$

where

$$u(\nu, T) = \frac{\partial}{\partial T} B_\nu(T), \tag{48}$$

and $B_\nu(T)$ is the Planck distribution. For instance, at $T = 2.5$ eV, the peak of the Rosseland weighting distribution is around 10 eV—the location of the unperturbed H I Lyα line. It is clear that the reduction in the depth of the resonances will impact the Rosseland mean. The inclusion of the motional

TABLE I. Comparison of the TR sum rule under different approximations at $B = 400$ MG (white dwarf application) for circularly polarized light: $q = 1$ and $q = -1$.

State	Field free	$K = 0$	$K = 20$
		$q = 1$	
$1s_{m=0}$	1.0	1.1610	1.1610
$2p_{m=-1}$	0.0	1.0728	1.0752
$2p_{m=0}$	1.0	1.5836	1.5840
$2s_{m=0}$	1.0	2.0143	2.0138
$3d_{m=-2}$	−1.0	1.1997	1.2047
		$q = -1$	
$1s_{m=0}$	1.0	0.8390	0.8390
$2p_{m=-1}$	2.0	0.9272	0.9248
$2p_{m=0}$	1.0	0.4164	0.4160
$2s_{m=0}$	1.0	−0.0143	−0.0138
$3d_{m=-2}$	3.0	0.7953	0.8003

Stark effect will therefore raise the Rosseland mean opacity compared to the case of static atoms.

Within the discussion about the effect of this work on opacity, it is important to also draw attention to the Thomas-Reiche-Kuhn (TRK) oscillator-strength sum rule. In the absence of a magnetic field, it is well known that the total oscillator strength out of a given level is equal to the number of electrons in that system [3]. For hydrogen, then the TRK sum rule states that

$$\sum_j f_{i\to j} = 1. \tag{49}$$

The TRK sum therefore places limits the total integrated opacity. However, in a magnetic field, the sum rules are modified and are a function of the magnetic field strength [33–35]

$$\sum_j f_{i\to j} = 1 + qL_z + q\frac{\beta}{2}\langle r_\perp^2\rangle, \tag{50}$$

where q is the polarization of the transition and L_z is the z component of angular momentum. Here, it is clear that the total integrated opacity will increase with magnetic-field strength. In the absence of a magnetic field, the TRK sum rule [Eq. (49)] is derived using simple operator relationships and is independent of the choice of the potential. However, with a magnetic field [Eq. (50)], the sum rule now depends on the specific state of the wave functions. Because the wave-function solution is modified by the motional Stark effect, it therefore also has an impact on the oscillator strength sum rule. These changes are two-fold: first, when a perpendicular electric field is applied, L_z is no longer an eigenstate of the new wave functions and will be modified from its static picture; second, the electric field causes elongation of the wave function in the x-y plane causing changes in the expectation value of $r_\perp^2$. If we consider the white dwarf case, where $B =$ 400 MG, overall, the motional Stark effect does not induce major changes in the TRK sum rule, though it is not fixed. We highlight some results in Table I for white dwarfs at $B = 400$ MG and in Table II for neutron stars at $B = 2.35 \times 10^{12}$ G.

TABLE II. Comparison of the TRK sum rule under different approximations at $B = 2.35 \times 10^{12}$ G (neutron star application) for circularly polarized light: $q = 1$ and $q = -1$.

State	$K = 0$	$K = 20$	$K = 100$
		$q = 1$	
$1s_{m=0}$	1.9963	1.9964	1.9972
$2p_{m=-1}$	1.9978	1.9978	1.9981
$3d_{m=-2}$	1.9983	1.9984	1.9982
		$q = -1$	
$1s_{m=0}$	0.0037	0.0036	0.0028
$2p_{m=-1}$	0.0022	0.0022	0.0019
$3d_{m=-2}$	0.0017	0.0016	0.0015

VII. CONCLUSION

It is well known that atoms moving in a magnetic field results in changes to the electronic energy structure; this phenomenon is known as the motional Stark effect. The impact of the motional Stark effect has been well documented for bound-state problems where states normalize to unity. However, the extension of the motional Stark effect to continuum problems is not trivial due to the delta function normalization. We present here a means of calculating the motional Stark effect on continuum problems by using a scattering formalism.

Our principal results are documented in Sec. V. To summarize, the motional Stark effect on continuum states does not strongly depend on the phase shift, transitions to $m = 1$ are less affected by motional Stark, resonances are shifted in energy (some up and some down), and other resonances appear at different values of atomic momenta. Taking the thermal average of these effects produces resonances in the continuum that become weaker and less distinct. Further, much of the structure disappears entirely.

The work presented here describes the most physically comprehensive bound-free opacity for atoms in a large magnetic field embedded in a thermal plasma. This work will be most significant for astrophysical plasmas, such as those found in the atmospheres of white dwarfs and neutron stars.

ACKNOWLEDGMENTS

T.A.G. acknowledges support from the George Ellery Hale Post-Doctoral Fellowship at the University of Colorado. J.W. acknowledges support from the United States Department of Energy National Nuclear Security Administration SSGF program under DE-NA0003960. M.C.Z. and C.J.F. acknowledge support from the Los Alamos National Laboratory (LANL) ASC PEM Atomic Physics Project. LANL is operated by Triad National Security, LLC, for the National Nuclear Security Administration of the U.S. Department of Energy under Contract No. 89233218NCA000001. I.B. acknowledges the Australian Research Council and the support of the National Computer Infrastructure and the Pawsey Supercomputer Centre.

APPENDIX: SCATTERING PROBLEM

The technique that we propose here involves the use of Green's functions within the scattering formalism [19,20]. In the scattering problem, the Schrödinger equation can be written in the form

$$(E - H)|\Psi\rangle = 0, \tag{A1}$$

where $|\Psi\rangle$ is the total scattering wave. The Lippmann-Schwinger equation can be readily derived [36] in the form

$$|\Psi\rangle = |\phi\rangle + \frac{1}{E - H_0} V|\Psi\rangle, \tag{A2}$$

where the second term is an in-coming or out-going scattered wave. In a magnetic field, the geometry is changed to being an effective one-dimensional problem. Therefore, rather than an in-coming or out-going wave, this same equation now becomes a reflected or transmitted wave.

The quantity $(E - H_0)^{-1}$ is often referred to as a Green's function, generally labeled as $\mathcal{G}$. The Green's function contains a singularity and is evaluated using complex analysis by introducing a small imaginary part

$$\lim_{\eta\to 0} \frac{1}{E - H_0 + i\eta} = \frac{\text{p.v.}}{E - H_0} - i\pi\delta(E - H_0), \tag{A3}$$

where p.v. denotes taking the Cauchy principal value. From here on out, as well as in the main text, the small imaginary part will be implied. We make a point of explicitly showing the delta function here as it will be important for the evaluation of the motional Stark effect.

An alternative to Eq. (A2) is to solve for the T matrix. The T matrix is defined as

$$T(E) = V + V\mathcal{G}T(E) \tag{A4}$$

and modifies the scattering equation to become

$$|\Psi\rangle = |\phi\rangle + \mathcal{G}T(E)|\phi\rangle. \tag{A5}$$

For this work, the T matrix is obtained by solving linear systems of the generic form $Ax = b$ [24]. The system to be solved is

$$[1 - V\mathcal{G}]T(E) = V, \tag{A6}$$

where the quantity in brackets corresponds to the matrix A, the T-matrix corresponds to x and V is the set of b.

For the motional Stark part of the problem, we have two potentials, i.e.,

$$H = H_0 + V_1 + V_2. \tag{A7}$$

In Refs. [20,36], a formalism was developed to address this problem. Within scattering, this approach appears in the context of a distorted-wave treatment, but proves to be advantageous for the specific problem at hand. In the case of a free electron in the potential of an atomic nucleus, V_2 can represent part of that potential, and V_1 can represent the motional Stark effect. The scattering problem then becomes one of finding a solution to the equation

$$|\Psi\rangle = |\phi\rangle + \frac{1}{E - H'} V_1|\Psi\rangle, \tag{A8}$$

where we define

$$H' = H_0 + V_2. \tag{A9}$$

For the motional Stark problem, H' does not have a known solution and is *not* diagonal in the $|knm\rangle$ basis, though H_0 will be diagonal in that given basis set.

[1] H. Ruder, G. Wunner, H. Herold, and F. Geyer, *Atoms in Strong Magnetic Fields. Quantum Mechanical Treatment and Applications in Astrophysics and Quantum Chaos* (Springer, Berlin, 1994).
[2] B. R. Johnson, J. O. Hirschfelder, and K.-H. Yang, Rev. Mod. Phys. **55**, 109 (1983).
[3] H. A. Bethe and E. E. Salpeter, *Quantum Mechanics of One- and Two-Electron Atoms* (Springer, New York, 1957).
[4] D. Baye and M. Vincke, Phys. Rev. A **42**, 391 (1990).
[5] G. G. Pavlov and P. Meszaros, Astrophys. J. **416**, 752 (1993).
[6] V. G. Bezchastnov and G. G. Pavlov, Phys. Rev. A **95**, 062512 (2017).
[7] A. Y. Potekhin, J. Phys. B: At. Mol. Opt. Phys. **27**, 1073 (1994).
[8] K. Mori and C. J. Hailey, Astrophys. J. **648**, 1139 (2006).
[9] J. Rosato, J. Quant. Spectrosc. Radiat. Transfer **306**, 108628 (2023).
[10] T. A. Gomez, M. C. Zammit, C. J. Fontes, and J. R. White, Astrophys. J. **951**, 143 (2023).
[11] T. A. Gomez, M. C. Zammit, I. Bray, C. J. Fontes, and J. R. White, Astrophys. J. **963**, 62 (2024).
[12] A. Y. Potekhin, Astronomy Astrophys. **518**, A24 (2010).
[13] L. B. Zhao, K. D. Wang, and K. Bartschat, Phys. Rev. A **103**, 022807 (2021).
[14] C. W. Clark, Phys. Rev. A **28**, 83 (1983).
[15] The energy of states in this representation does not depend on the s quantum number.
[16] W. Roesner, G. Wunner, H. Herold, and H. Ruder, J. Phys. B: Atom. Mol. Phys. **17**, 29 (1984).
[17] A. Y. Potekhin, G. G. Pavlov, and J. Ventura, Astronomy Astrophys. **317**, 618 (1997).
[18] A. Y. Potekhin and G. G. Pavlov, Astrophys. J. **483**, 414 (1997).
[19] B. A. Lippmann and J. Schwinger, Phys. Rev. **79**, 469 (1950).
[20] N. F. Mott and H. S. W. Massey, *The Theory of Atomic Collisions* (Clarendon, Oxford, 1949).
[21] B. L. Moiseiwitsch and S. J. Smith, Rev. Mod. Phys. **40**, 238 (1968).
[22] G. Wunner, H. Ruder, and H. Herold, Phys. Lett. A **79**, 159 (1980).
[23] H. Herold, H. Ruder, and G. Wunner, J. Phys. B: At. Mol. Phys. **14**, 751 (1981).
[24] I. Bray and A. T. Stelbovics, Phys. Rev. A **46**, 6995 (1992).

[25] E. Luc-Koenig and A. Bachelier, J. Phys. B: At. Mol. Phys. **13**, 1743 (1980).
[26] F. Hardy, P. Dufour, and S. Jordan, MNRAS **520**, 6111 (2023).
[27] F. K. Lamb and P. G. Sutherland, in *Physics of Dense Matter*, Vol. 53, edited by C. J. Hansen (Cambridge University Press, Cambridge, England, 1974), p. 265.
[28] S. Jordan, Astronomy Astrophys. **265**, 570 (1992).
[29] P. Dufour (private communication, 2024).
[30] G. D. Schmidt, S. C. West, J. Liebert, R. F. Green, and H. S. Stockman, Astrophys. J. **309**, 218 (1986).
[31] B. T. Gänsicke, G. D. Schmidt, S. Jordan, and P. Szkody, Astrophys. J. **555**, 380 (2001).
[32] I. Hubeny and D. Mihalas, *Theory of Stellar Atmospheres* (Princeton University Press, Princeton, NJ, 2014).
[33] H. Hasegawa and R. E. Howard, J. Phys. Chem. Solids **21**, 179 (1961).
[34] G. Wunner and H. Ruder, Astrophys. J. **242**, 828 (1980).
[35] J. M. Wadehra, Astrophys. J. **248**, 874 (1981).
[36] M. Gell-Mann and M. L. Goldberger, Phys. Rev. **91**, 398 (1953).